

Geophysical Research Letters[®]



RESEARCH LETTER

10.1029/2025GL115606

Key Points:

- Since 1975, sediment accumulation in the inner Gulf of Thailand (IGoT) increased from 20.8 to 29.5 Mt/yr but riverine fluxes decreased from 6.6 to 5.4 Mt/yr
- Coastal erosion contributes significantly to IGoT sediment accumulation but the eroded coastal organic carbon has a low burial efficiency ($16.8 \pm 5.5\%$)
- Global mangrove loss could contribute ~ 175 Tg/yr CO_2 , making preserving coastal ecosystems critically important

Supporting Information:

Supporting Information may be found in the online version of this article.

Correspondence to:

B. Wei,
bingbing.wei@awi.de

Citation:

Wei, B., Kusch, S., Hanebuth, T. J. J., Hu, L., Fan, M., Jia, G., et al. (2025). Coastal erosion as a major sediment source in the inner Gulf of Thailand: Implications for carbon dynamics in tropical coastal ocean systems. *Geophysical Research Letters*, 52, e2025GL115606. <https://doi.org/10.1029/2025GL115606>

Received 25 FEB 2025

Accepted 13 MAY 2025









Author Contributions:

Conceptualization: Bingbing Wei, Stephanie Kusch
Formal analysis: Bingbing Wei, Stephanie Kusch, Miao Fan
Funding acquisition: Bingbing Wei, Moritz Holtappels
Investigation: Bingbing Wei, Till J. J. Hanebuth, Limin Hu
Writing – original draft: Bingbing Wei
Writing – review & editing: Stephanie Kusch, Till J. J. Hanebuth, Limin Hu, Miao Fan, Guodong Jia, Gesine Mollenhauer, Moritz Holtappels

© 2025. The Author(s).

This is an open access article under the terms of the [Creative Commons Attribution License](#), which permits use, distribution and reproduction in any medium, provided the original work is properly cited.

Coastal Erosion as a Major Sediment Source in the Inner Gulf of Thailand: Implications for Carbon Dynamics in Tropical Coastal Ocean Systems

Bingbing Wei^{1,2} , Stephanie Kusch³ , Till J. J. Hanebuth⁴ , Limin Hu^{5,6} , Miao Fan⁷ , Guodong Jia⁸ , Gesine Mollenhauer^{1,2,9} , and Moritz Holtappels^{1,2} 

¹Alfred Wegener Institute, Helmholtz Center for Polar and Marine Research, Bremerhaven, Germany, ²MARUM—Center for Marine Environmental Sciences, University of Bremen, Bremen, Germany, ³ISMER Institute of Marine Sciences, University of Quebec Rimouski, Rimouski, QC, Canada, ⁴Department of Marine Science, Coastal Carolina University, Conway, SC, USA, ⁵College of Marine Geosciences, Chongben Honors College, Key Laboratory of Submarine Geosciences and Technology, Ocean University of China, Qingdao, China, ⁶Laboratory for Marine Geology, Qingdao Marine Science and Technology Center, Qingdao, China, ⁷National Marine Data and Information Service, Tianjin, China, ⁸State Key Laboratory of Marine Geology, Tongji University, Shanghai, China, ⁹Department of Geosciences, University of Bremen, Bremen, Germany

Abstract Coastal erosion is an increasingly dominant sediment source in marginal seas, particularly in low-lying areas affected by deltaic subsidence and sediment deficits from upstream water management. However, its role in sediment and organic carbon (OC) dynamics remains to be estimated. Our analyses of the inner Gulf of Thailand (IGoT) revealed that riverine sediment fluxes decreased from 6.6 to 5.4 Mt/yr after 1975, while sediment accumulation within the IGoT increased from 20.8 to 29.5 Mt/yr. The observed trend indicates major sediment contributions from coastal erosion, particularly from mangrove deposits. This process destabilizes coastal ecosystems and accelerates OC decomposition, that is, a low burial efficiency ($16.8 \pm 5.5\%$) leads to CO_2 release. Extrapolating these findings globally, mangrove loss could release ~ 175 Tg/yr CO_2 . As coastal erosion intensifies under sea-level rise and human land-use practices, preserving coastal ecosystems is critical for mitigating blue carbon loss and maintaining coastal stability and resilience.

Plain Language Summary Coastal areas are increasingly eroding due to rising sea levels, reduced riverine sediment supply, and deltaic subsidence. The impact on global and regional carbon dynamics remains poorly resolved although the carbon cycle is closely tied to a changing climate and human land-use practices. In the inner Gulf of Thailand, riverine sediment discharge has decreased from 6.6 to 5.4 Mt/yr since 1975 because of upstream river damming and field irrigation management. However, the total sediment accumulation within the inner gulf is much higher than the river input and has also increased from 20.8 to 29.5 Mt/yr during the same time. This discrepancy indicates that coastal erosion, especially of mangrove deposits, is now a major source of sediment and organic carbon. However, the organic carbon freshly from eroded coastal mangrove deposits decomposes significantly, releasing carbon dioxide into the atmosphere. Based on these findings, global mangrove loss could emit around 175 million tons carbon dioxide per year. As sea level rises and human land-use practices intensify, protecting coastal ecosystems is crucial to prevent further carbon loss and maintain stable shorelines.

1. Introduction

Coastal environments are dynamic interfaces between land and sea, supporting critical infrastructure, ecosystems and nearly 40% of the global population (Martínez et al., 2007). These dynamic systems constantly evolve as rivers, nearshore currents, and waves transport and circulate sediment within and beyond nearshore areas (Mentaschi et al., 2018). However, specifically the low-lying coasts face increasing threats from human activities, land subsidence, eustatic sea-level rise, and atmospheric-hydrological effects of a changing climate (Barnard et al., 2015; Darby et al., 2016; Syvitski et al., 2009). Coastal Asia has been particularly affected, losing 5,940 km² of area to erosion between 1984 and 2015, which accounts for 42% of the global coastal area loss of 14,050 km² (Figure 1a; Mentaschi et al., 2018). The low-lying river deltas and their adjacent coastal regions, such as the Yellow, Yangtze, Mekong, and Chao Phraya mega-deltas, are particularly vulnerable to shoreline retreat and erosion due to their low elevation, subsidence, riverine sediment reduction from damming, and sea level rise

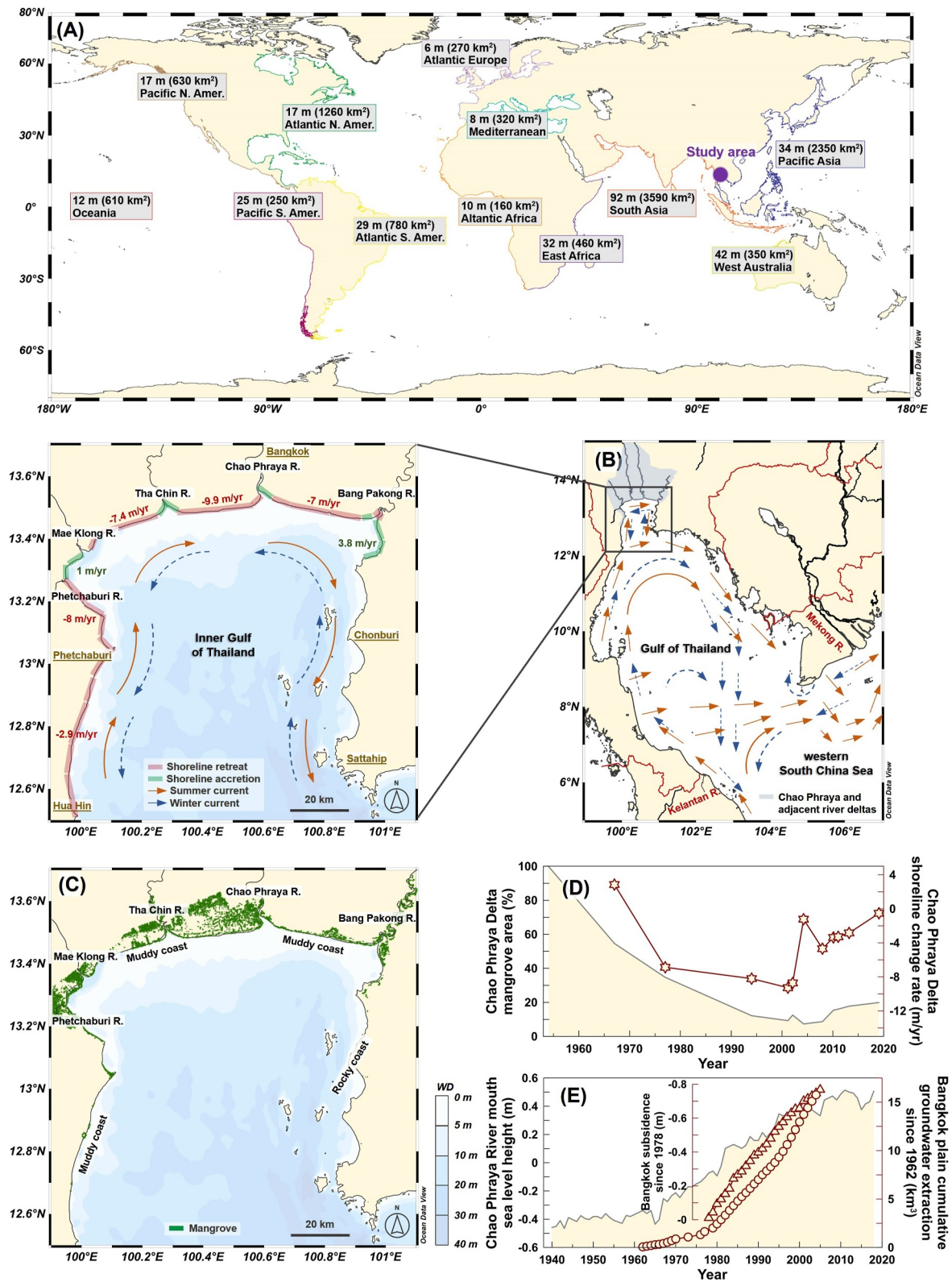


Figure 1.

(Syvitski et al., 2009). Despite advances in the study of shoreline evolution, the redistribution and fate of eroded sediments within shallow-marine environments remain poorly understood (Wagner et al., 2024). Coastal-tidal ecosystems, including mangroves, salt marshes, and seagrass beds, are important “blue carbon” ecosystems, storing 14–25.3 Pg C in their top meter soils and contributing 47% of total carbon burial in ocean sediments (Duarte et al., 2013). However, coastal erosion can remobilized and degraded this stored carbon, releasing CO₂ and weakening the carbon sink function of coastal zones (e.g., Adame et al., 2021). The extent of this positive feedback depends on the poorly constrained proportion between degradation and burial of the eroded carbon in marine sediments.

The inner Gulf of Thailand (IGoT) is among the regions facing significant pressure from climate change and human activities. For instance, relative sea-level rise in the region has reached 1.4 cm/yr over the past 80 years, nearly five times the global average of ~0.3 cm/yr (Figure 1e; Bidorn et al., 2021). Since 1975, sustained high groundwater extraction rates driven by rapid socio-economic growth in Thailand, have caused ~0.8 m of land subsidence in the Chao Phraya and adjacent deltas (Figure 1e; Lorphensri et al., 2011; Phien-wej et al., 2006). Meanwhile, sediment supply to the Chao Phraya Delta has halved since the 1960s due to upstream water management, a trend common across Southeast Asia (Bidorn et al., 2023). These factors have led to shoreline retreat of 7–10 m/yr along the northern coast and 3–8 m/yr along the western coast of the IGoT, except near active river mouths where sediment supply enables accretion of 1–4 m/yr (Figures 1b and 1c; Bidorn et al., 2021; Sok et al., 2022). Subaerial and subaqueous deltaic subsidence has deepened nearshore waters, allowing stronger waves to reach the coast with less energy loss, thus intensifying coastal erosion through stronger wave action and sediment transport (Nutalaya, 1996; Saito, 2000). Widespread mangrove loss across subaerial deltaic plains (Figures 1c and 1d; Bidorn et al., 2021) has further reduced coastal resilience, accelerating erosion by weakening natural defences against waves, coastal currents, and storm surges (Vongvisessomjai et al., 1996).

The IGoT provides a valuable example to investigate the impacts of coastal erosion on sediment redistribution and carbon dynamics under climate change and extended anthropogenic activities. This region benefits from extensive data on riverine sediment and organic carbon (OC) input, time-series of sediment and OC accumulation, $\delta^{13}\text{C}$ -based source tracing, and detailed sediment transport and depositional processes (e.g., Bai et al., 2021; Bidorn et al., 2023; Windom et al., 1984; Wu et al., 2020). Also, the IGoT is fed by one of the Asian mega-deltas, the Chao Phraya, and is a semi-closed, funnel-shaped, and shallow epicontinental shelf sea, amplifying the input-erosional-depositional dynamics. This study integrates and reanalyzes existing data sets to assess the links between coastal erosion, offshore sediment redistribution, and OC budget, focusing on the balance between OC loss and burial. The findings shed light on the long-term effect of coastal erosion on carbon cycling and its broader implications for global carbon dynamics.

2. Material and Methods

2.1. Study Area

The Gulf of Thailand (GoT) is a shallow epicontinental gulf opening eastward into the western South China Sea. Its innermost region, the IGoT, covers ~10,000 km² with an average water depth of 15 m and a maximum of 40 m (Figure 1b). The IGoT primarily receives riverine sediments from the Chao Phraya River in the north, with minor contributions from the Phetchaburi, Mae Klong, Tha Chin, and Bang Pakong Rivers (Figure 1b, Table 1). Riverine sediment input has sustained shoreline accretion of 15 m/yr over the past 6,000 years, despite the retreat in the last century (Saito, 2000). The region experiences a seasonal climate with a warm, wet southwest monsoon in summer (May–September) and a cooler, dry northeast monsoon in winter (November–February), driving seasonal surface water circulation that flows clockwise in summer and reverses in winter (Anutaliya, 2023). Tides

Figure 1. (a) Global coastal land loss shown as linear distance and area for 1984–2015 (data from Mentaschi et al., 2018); (b) A map of the Gulf of Thailand showing surface currents (modified from Pa'suya et al., 2015) along with an inset illustrating shoreline retreat and accretion in the inner gulf between 1954 and 2019 (data compiled and replotted from Bidorn et al., 2021; Imlamai et al., 2023; Sok et al. (2022), and Vongvisessomjai et al., 1996); (c) Mangrove distribution in the inshore area of the IGoT in 2000 (data from Giri et al., 2011) and coastal bathymetry; (d) Changes in shoreline (stars, right scale) and relative mangrove coverage (normalized to the area in 1954, filled line, left scale) in the Chao Phraya Delta from 1954 to 2019 (data from Bidorn et al., 2021; Phien-wej et al., 2006); (e) Trends in annual sea level height (filled line, left scale) at the Chao Phraya River mouth, cumulative groundwater extraction (circles, right scale) in the Bangkok plain since 1962, and land subsidence (triangles, inset scale) in Bangkok after 1978 (data from Bidorn et al., 2021; Lorphensri et al., 2011; Phien-wej et al., 2006). The map was created using Ocean Data View software (Schlitzer, 2018).

Table 1
Sediment and OC Budget in the IGoT for the Pre- and Post-1975 Periods

Sediment accumulation and OC burial fluxes in the IGoT												
Sediment (pre-1975)					Sediment (post-1975)			OC _{river} (post-1975)			OC _{coastal} (post-1975)	
		Terrigenous sediment accumulation flux (Mt/yr)		MAR ^a (g/cm ² /yr)	Terrigenous sediment accumulation flux (Mt/yr)		Content ^b (wt.%)	Burial flux (Gg/yr)	Burial rate (g/m ² /yr)	Content ^b (wt.%)	Burial flux (Gg/yr)	Burial rate (g/m ² /yr)
Area (km ²)	CaCO ₃ + BSi-m (wt.%)	MAR ^a (g/cm ² /yr)	Terrigenous sediment flux (Mt/yr)	MAR ^a (g/cm ² /yr)	Content ^b (wt.%)	Burial flux (Gg/yr)	Burial rate (g/m ² /yr)	Content ^b (wt.%)	Burial flux (Gg/yr)	Content ^b (wt.%)	Burial flux (Gg/yr)	Burial rate (g/m ² /yr)
Zone												
A	2,650	11.8 ± 1.18	0.33	7.7 ± 0.8	0.60	15.9 ± 1.6	0.30	47.7 ± 4.8	18.0	0.35	55.7 ± 5.6	21
B	7,210	17.8 ± 1.78	0.22	13.0 ± 1.3	0.26	18.7 ± 1.9	0.08	15 ± 1.5	2.1	0.11	20.6 ± 2.1	2.9
Total	9,860			20.8 ± 1.6		29.5 ± 2.1		62.7 ± 5.0	6.4 ± 0.5		76.3 ± 6.0	7.7 ± 0.6
Sediment and OC input fluxes from main rivers												
Sediment input flux (pre-1975, Mt/yr)					Sediment input flux (post-1975, Mt/yr)			OC _{river} input (post-1975) OC _{coastal} input (post-1975)				
River	Basin area (10 ³ km ²) ^b	CaCO ₃ -r (wt.%)	Discharge (pre-1975, km ³ /yr)	Terrigenous sediment	Total sediment	Discharge (post-1975, km ³ /yr)	Terrigenous sediment	Total sediment	Content ^c (wt.%)	flux (Gg/yr)	Content (wt.%)	Flux (Gg/yr)
			1. Phetchaburi	2. Mae Klong	3. Tha Chin	4. Chao Phraya	5. Bang Pakong					
1. Phetchaburi	6	4.1	0.9 ± 0.4	0.3 ± 0.1	0.3 ± 0.1	0.4 ± 0.2	0.1 ± 0.1	0.1 ± 0.1	2.9 ± 0.2	4.0 ± 0.2		
2. Mae Klong	31	4.1	12.7 ± 3.0	0.8 ± 0.2	0.8 ± 0.2	7.1 ± 2.5	0.4 ± 0.2	0.4 ± 0.2	2.9 ± 0.2	12.9 ± 0.8		
3. Tha Chin	14	4.2	0.4 ± 0.2	0.1 ± 0.1	0.1 ± 0.1	0.2 ± 0.1	0.1 ± 0.0	0.0 ± 0.0	5.6 ± 0.1	3.0 ± 0.1		
4. Chao Phraya	160	2.8	26.2 ± 7.6	4.9 ± 1.4	4.8 ± 1.3	22.1 ± 8.8	4.5 ± 3.3	4.4 ± 3.3	3.9 ± 0.1	174.6 ± 5.3		
5. Bang Pakong	10	1.7	4.8 ± 1.4	0.7 ± 0.2	0.7 ± 0.2	3.3 ± 1.0	0.5 ± 0.2	0.5 ± 0.2	2.4 ± 0.0	12.3 ± 0.0		
Total riverine input flux			44.9 ± 7.7	6.9 ± 1.4	6.7 ± 1.3	33.1 ± 8.8	5.6 ± 3.4	5.5 ± 3.3		186.9 ± 5.4		
Coastal input flux					14.0 ± 2.1^d						1.8 ± 0.6	452.9 ± 142.8^e

Note. The main results in the table are highlighted in bold. ^aMAR of total sediments in the IGOT pre-1975 and post-1975 was calculated using published MAR data (Figure 2a). ^bThe contents of OC_{river} and OC_{coastal} in Zones A and B are averaged based on values calculated using three-endmember mixing model (Section 2.3, Figures 2h and 2i). ^cThe input OC_{river} content for each river are calculated based on values from Ubonyiem et al. (2023). ^dThe coastal sediment input flux is calculated by subtracting riverine terrigenous sediment input flux from total terrigenous sediment accumulation flux for the pre-1975 and post-1975 periods. ^eThe OC_{coastal} input flux is calculated by multiplying the averaged OC_{coastal} content in coastal mangrove deposits in the region (data sources in Table S5 in Supporting Information S1) by the coastal sediment input flux.

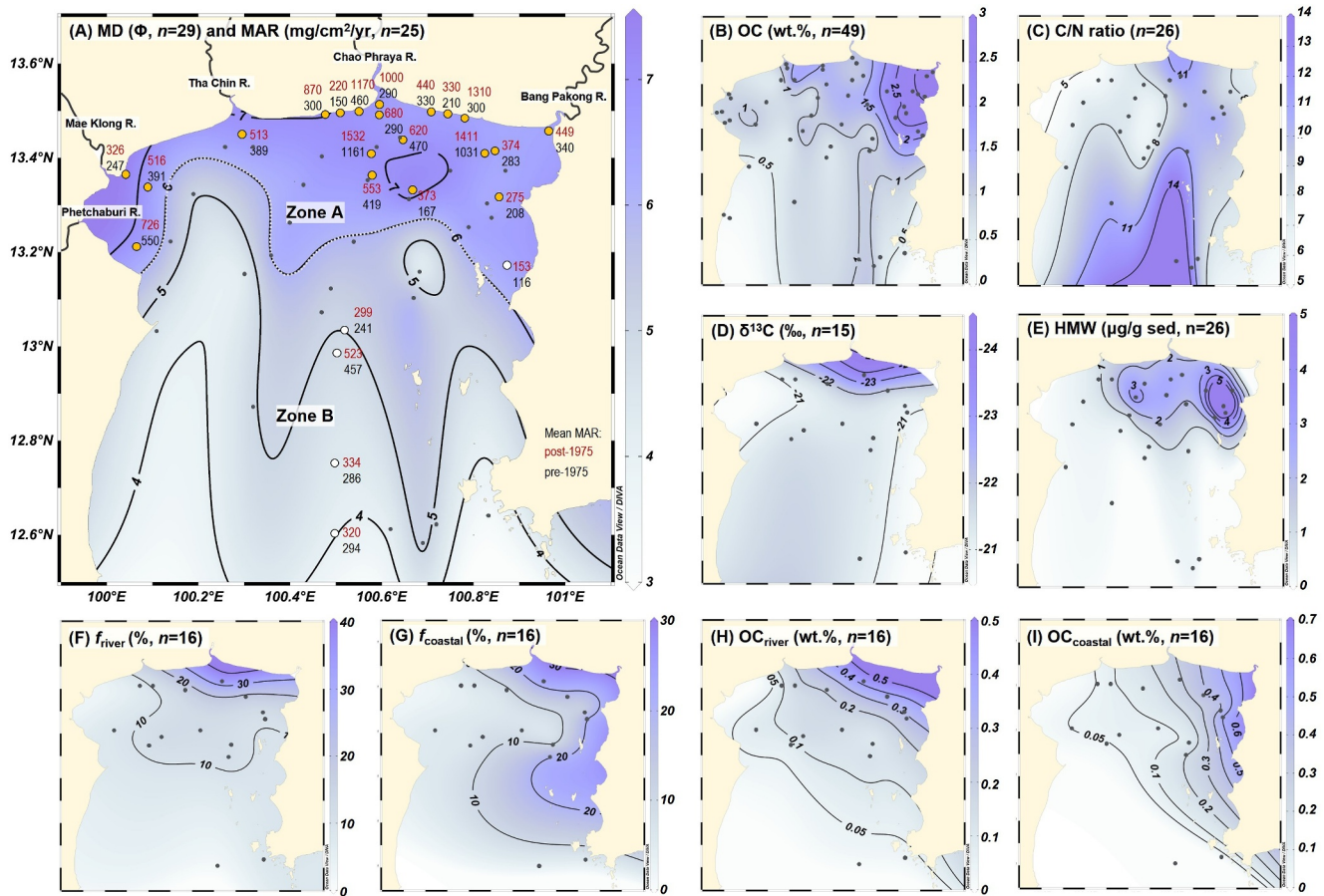


Figure 2. Spatial distribution of (a) median grain size (MD, Φ , contour lines) and mass accumulation rates (MAR) pre- and post-1975 (yellow dots in Zone A, white dots in Zone B; black and red numbers represent MAR pre-1975 and post-1975, respectively), (b) bulk OC contents, (c) C/N ratios, (d) $\delta^{13}\text{C}$ values of bulk OC, (e) HMW n -alkane abundances, (f) proportion of OC_{river} , (g) proportion of $\text{OC}_{\text{coastal}}$, (h) OC_{river} contents, and (i) $\text{OC}_{\text{coastal}}$ contents in surface sediments of the IGoT. MAR data in panel (a) are provided in Table S2 in Supporting Information S1, and data for panels (a–e) are sourced from Bai et al. (2021) and Lin et al. (2023). In panel (a), the boundary between Zones A and B is defined by the MD contour line of Φ 6 (dotted black line). The map was generated using Ocean Data View software (Schlitzer, 2018). Sampling stations for panels (a–i) are marked as small black dots, with station numbers indicated in the respective captions.

in the region are semi-diurnal, ranging from 1.5 m (neap) to 2.5 m (spring), generating weak tidal currents (<0.25 m/s; JICA, 2000).

2.2. Data Collection and Harmonization

Discharge and suspended sediment flux data for the five main rivers draining into the IGoT were obtained from hydrological stations (Thailand Hydrological Yearbook, 1912–2020; Texts S1–S5 and Figures S1–S5 in Supporting Information S1). While bedload data are scarce, Bidorn et al. (2023) performed direct measurements and showed that bedload accounts for $\sim 5\%$ of suspended load in the Chao Phraya River, a proportion incorporated into our total sediment flux calculations. To ensure consistency and alignment with sediment accumulation rates in the IGoT, river discharge and total sediment flux data were analyzed separately for pre-1975 (1930–1974) and post-1975 (1975–2020) periods and calculated averages accordingly (Texts S1–S5 in Supporting Information S1).

Sediment accumulation rates taken from previous studies (Table S1 in Supporting Information S1) generally represent multi-decade averages with varying time spans across stations. Although studies on historical changes in linear sedimentation rate (LSR) or mass accumulation rate (MAR) over the past century are limited, available data indicates a clear increase after 1975 (Figure 2a; Table S1 in Supporting Information S1), with MARs rising on average by a factor of 2.5 in nearshore cores and 1.3 in offshore cores (Figure S7 and Table S2 in Supporting Information S1) (Bidorn et al., 2021; Boonyatumanond et al., 2007; Chaisanguansuk et al., 2023; Cheevaporn

et al., 1994; Guo et al., 2018; Srisuksawad et al., 1997; Windom et al., 1984). These factors were applied to all sediment cores in areas with reported historical changes in LSR or MAR, ensuring consistency across sites and alignment with river sediment flux data. The selection of 1975 as a boundary year is further justified by significant environmental and anthropogenic shifts during this period, including extensive mangrove deforestation, accelerated sea-level rise, and sustained high groundwater extraction rates (Figures 1d and 1e), all of which have impacted sediment dynamics, land subsidence, and OC burial in the IGoT (Bidorn et al., 2021; Phien-wej et al., 2006).

Geochemical properties of surface sediments (0–3 or 0–5 cm intervals), including median grain size, OC contents, C/N ratios, $\delta^{13}\text{C}$ values of OC, and high-molecular-weight (C_{23-35} , HWM) *n*-alkanes abundances, were compiled from previous studies (Bai et al., 2021; Lin et al., 2023).

2.3. Source Apportionment Calculations

A three end-member mixing model using $\delta^{13}\text{C}$ values and C/N ratios of bulk OC was applied to quantify the contributions of marine ($\text{OC}_{\text{marine}}$, f_{marine}), riverine (OC_{river} , f_{river}) and coastal ($\text{OC}_{\text{coastal}}$, f_{coastal}) OC sources in IGoT sediments:

$$f_{\text{marine}} \times \delta^{13}\text{C}_{\text{marine}} + f_{\text{river}} \times \delta^{13}\text{C}_{\text{river}} + f_{\text{coastal}} \times \delta^{13}\text{C}_{\text{coastal}} = \delta^{13}\text{C}_{\text{OC}} \quad (1)$$

$$f_{\text{marine}} \times (C/N)_{\text{marine}} + f_{\text{river}} \times (C/N)_{\text{river}} + f_{\text{coastal}} \times (C/N)_{\text{coastal}} = (C/N)_{\text{OC}} \quad (2)$$

$$f_{\text{marine}} + f_{\text{river}} + f_{\text{coastal}} = 1 \quad (3)$$

where $\text{OC}_{\text{marine}}$ was assigned a $\delta^{13}\text{C}$ value of $-21.5 \pm 0.4\text{‰}$ and a C/N ratio of 5.7 ± 0.4 , based on measurements from the central IGoT (Boonphakdee et al., 2008; Thimdee et al., 2003); OC_{river} has a $\delta^{13}\text{C}$ value of $-26.3 \pm 0.6\text{‰}$ and a C/N ratio of 11.7 ± 1.2 representing the composition of sediments from the five IGoT rivers (Table S4 in Supporting Information S1; Narman, 2020); $\text{OC}_{\text{coastal}}$ is assigned a $\delta^{13}\text{C}$ value of $-26.2 \pm 0.5\text{‰}$ and a C/N ratio of 16.4 ± 1.3 , based on mangrove deposits (soil, leaves and roots) (Table S4 in Supporting Information S1). A Bayesian Markov chain Monte Carlo (MCMC) simulation was performed in Matlab (R2015a, MathWorks, USA) to account for end-member variability and estimated uncertainties in the calculated OC fractions (Bosch et al., 2015). From 10^8 random samples, 10^6 were selected based on mean and standard deviations from the normal distribution to meet system constraints. Mean and standard deviations of each OC source contribution were determined (Bosch et al., 2015), and the $\text{OC}_{\text{marine}}$, OC_{river} , and $\text{OC}_{\text{coastal}}$ contents were calculated by multiplying bulk OC content with the respective source proportions at each station.

2.4. Sediment and OC Flux Calculations

Our meta-analysis of surface sediments (0–3 or 0–5 cm, representing deposition intervals from the past few years to three decades, primarily within the post-1975 period) revealed spatial heterogeneity in key parameters across the IGoT, which we use for the definition of sedimentation zones as follows. Median grain size (ϕ , $\Phi = -\log_2(d)$ with d being the grain diameter in mm) ranged from Φ 3 to 7, peaking at Φ 6–7 near rivers mouths and in the northeast (Figure 2a). OC content varied from 0.23 to 2.93 wt.%, with highest values near the Bang Pakong River mouth in the northeast (Figure 2b). The C/N ratio was >11 in the central southern part, 8–11 in the northeastern part, and <8 elsewhere (Figure 2c). $\delta^{13}\text{C}$ values of OC ranged from -24.2‰ to -21.45‰ , with more negative values near the Chao Phraya and Bang Pakong river mouths (Figure 2d). HMW *n*-alkane abundance, an indicator of terrestrial OC input, was also highest near these two river mouths ($1\text{--}18.5 \mu\text{g/g}$ sed) and lower elsewhere ($0.1\text{--}1 \mu\text{g/g}$ sed; Figure 2e). Overall, median grain size, OC content, and HMW *n*-alkane abundance decrease southwestward, while $\delta^{13}\text{C}$ values of OC became less negative (Figures 2b and 2c). Based on these variabilities, two sedimentation zones were defined: (a) *Zone A* (the river mouths/northeastern IGoT) with fine sediments ($\Phi \geq 6$), high MARs, elevated OC_{river} and $\text{OC}_{\text{coastal}}$ contents, and high HMW *n*-alkane abundances, showing mudbelt characteristics; and (b) *Zone B* (remaining areas) with coarser sediment ($\Phi < 6$), low MARs, reduced OC_{river} and $\text{OC}_{\text{coastal}}$ contents, and low *n*-alkane abundances (Figures 2a, Table 1). Further details on OC_{river} and $\text{OC}_{\text{coastal}}$ are provided in the Results.

Accumulation fluxes for total sediment, terrigenous sediments (excludes carbonate and biogenic silica), and burial flux for OC_{river} and $\text{OC}_{\text{coastal}}$ were calculated as follows:

$$\text{Total sediment accumulation flux} = \text{MAR} \times [\text{area}] \quad (4)$$

$$\text{Terrigenous sediment accumulation flux} = \text{total sediment accumulation flux} \times (1 - f_{\text{CaCO}_3 \& \text{BSi-m}}) \quad (5)$$

$$\text{OC}_{\text{river}} \text{ burial flux} = \text{total sediment accumulation flux} \times \text{OC}_{\text{river}} \quad (6)$$

$$\text{OC}_{\text{coastal}} \text{ burial flux} = \text{total sediment accumulation flux} \times \text{OC}_{\text{coastal}} \quad (7)$$

where [area] is the area of zones A and B, and $f_{\text{CaCO}_3 \& \text{BSi-m}}$ is the proportion of carbonate and biogenic silica in IGoT sediments (averaging 11.75 wt.% in Zone A and 17.75 wt.% in Zone B; Hungspreugs et al., 2002; Sompongchaiyakul et al., 2019).

The terrigenous sediment input from rivers is calculated after removing terrigenous carbonate as:

$$\text{Total terrigenous sediment input flux} = \sum (\text{sediment input flux from each river} \times (1 - f_{\text{CaCO}_3-r})) \quad (8)$$

$$\text{Total OC}_{\text{river}} \text{ input flux} = \sum (\text{sediment input flux from each river} \times [\text{input OC}_{\text{river}}]) \quad (9)$$

where f_{CaCO_3-r} is the carbonate content in river sediments (1.7–4.1 wt.%, Ubonyaem et al., 2023), while biogenic silica is generally absent. The term [input OC_{river}] is the average OC content of suspended and bedload river sediments for each river, calculated as 95% of suspended OC content (~1.5× riverbed OC content; Wei et al., 2024) plus 5% of bedload OC content (generally comparable to riverbed OC content; Ubonyaem et al., 2023).

3. Results

From 1930 to 2020, the total annual water discharge from the five main rivers into the IGoT decreased from 44.9 ± 7.7 pre-1975 to 33.1 ± 8.8 km³/yr post-1975, and terrigenous sediment input flux decreased from 6.7 ± 1.3 to 5.5 ± 3.3 Mt/yr, with an increase of the contribution from the Chao Phraya River from 71% to 80% (Table 1). However, the total terrigenous sediment accumulation flux in the IGoT increased significantly from 20.8 ± 1.6 Mt/yr before 1975 to 29.5 ± 2.1 Mt/yr after 1975 (Table 1). After 1975, the five rivers contributed an average OC_{river} input flux of 186.9 ± 5.4 Gg/yr, based on stable input with OC_{river} contents of 2.9 ± 0.2 (Phetchaburi), 2.9 ± 0.2 (Mae Klong), 5.6 ± 0.1 (Tha Chin), 3.9 ± 0.1 (Chao Phraya), and 2.4 ± 0.0 (Bang Pakong) wt.% (Table 1; Ubonyaem et al., 2023). OC_{river} input flux pre-1975 could not be calculated due to the lack of input OC_{river} data for that time period.

The mixing model revealed that the IGoT surface sediments consist of 36%–88% OC_{marine}, 7%–39% OC_{river}, and 4%–25% OC_{coastal} (Figures 2f and 2g; Table S5 in Supporting Information S1). The corresponding contents ranged from 0.31 to 1.89 wt.% for OC_{marine}, 0.03 to 0.46 wt.% for OC_{river}, and 0.02 to 0.69 wt.% for OC_{coastal} (Figures 2h and 2i; Table S5 in Supporting Information S1). The spatial distribution of OC_{marine} proportions and contents, while shown in Figure S8 in Supporting Information S1, is beyond the scope of this study and is, therefore, not further considered here. Both OC_{river} and OC_{coastal} contents were highest in the northeastern IGoT, gradually decreasing southwestward (Figures 2h and 2i). For the post-1975 period, the average OC_{river} accumulation flux in Zone A (47.7 ± 4.8 Gg/yr) is 3 times higher than in Zone B (15 ± 1.5 Gg/yr, Table 1), and the average OC_{river} accumulation rate in Zone A (18.0 g/m²/yr) was 9 times higher than in Zone B (2.1 g/m²/yr, Table 1). Similarly, the average OC_{coastal} accumulation flux in Zone A (55.7 ± 5.6 Gg/yr) was 3 times higher than in Zone B (20.6 ± 2.1 Gg/yr), and the OC_{coastal} accumulation rate in Zone A (21 g/m²/yr) was 7 times higher than in Zone B (2.9 g/m²/yr, Table 1).

4. Discussion

4.1. Significant Sediment Input From Coastal Erosion Into the IGoT

An accurate sediment budget is essential for understanding source-to-sink dynamics in marginal seas and their variations under climatic and anthropogenic influences (Syvitski et al., 2022). However, this approach is often

impeded by limited data available on riverine sediment input fluxes and marine MAR records of terrigenous sediments (e.g., Liu et al., 2024; Tegler et al., 2024).

In this meta-analysis study, we precisely quantified total riverine sediment input fluxes (suspended and bedload) from the five main rivers draining into the IGoT (Texts S1–S5 and Figure S1–S5 in Supporting Information S1). Terrigenous sediment fluxes decreased from 6.7 ± 1.3 Mt/yr pre-1975 to 5.4 ± 3.3 Mt/yr post-1975 (Table 1), primarily due to upstream water management, such as the Chao Phraya, Bhumibol and Sirikit dams (Bidorn et al., 2023), which significantly reduced tributary sediment discharge to the delta. This decline was partially offset by increased sediment supply from the delta, driven by changes to more industrial land use that enhanced soil erosion (Bidorn et al., 2023; Sok et al., 2022). However, the accumulation flux of terrigenous sediment in the IGoT increased from 20.8 ± 1.6 Mt/yr ($3.0\times$ riverine supply) pre-1975 to 29.5 ± 2.1 Mt/yr ($5.2\times$ riverine supply) post-1975 (Table 1), indicating additional sediment inputs of 14.0 ± 2.1 and 24.0 ± 3.9 Mt/yr, respectively. Nearby small rivers are unlikely major contributors; although their sediment inputs are unknown, due to size we do not expect them to exceed the input of the Phetchaburi River (0.3 Mt/yr pre-1975 and 0.1 Mt/yr post-1975; Table 1). Similarly, distant large rivers (e.g., the Mekong, Kelantan, and Pahang Rivers) are unlikely contributing sources due to their $>1,000$ km distance from the IGoT, as noted also by Shi et al. (2015). Sediment grain size (Qiao et al., 2015) and clay mineral composition in the IGoT (15%–20% kaolinite and 50%–70% smectite) closely match those of the five main rivers draining into the IGoT (24%–40% kaolinite and 23%–58% smectite; Liu et al., 2016), with minor variations attributed to preferential flocculation and deposition of kaolinite near river mouths and offshore transport of smectite (Kessarkar et al., 2010; Liu et al., 2011; Wei et al., 2024). In contrast, Mekong sediments exhibit a distinctly different clay mineral composition (33%–42% illite, 27%–32% kaolinite, 20%–28% chlorite; Liu et al., 2016), confirming the absence of this sediment source. Local hydrodynamic regimes further influence the sediment distribution in the IGoT, similar to observations on the coastal Sunda Shelf off the Malay Peninsula (Wei et al., 2024). Strong vertical mixing generally occurs during the dry season (mainly Dec-Jan), facilitating the dispersal of OC by counterclockwise surface currents. However, in most years, a stratified water column limits this dispersal, favoring sediment retention in estuarine and inshore areas, particularly during the wet season when river input is high (Wu et al., 2020). As a result, Chao Phraya sediments primarily settle in the northeastern IGoT due to the topographically enclosed low-energy environment and clockwise summer current circulation that promotes sediment trapping (Shi et al., 2015; Windom et al., 1984; Wu et al., 2020).

Coastal erosion, therefore, is the most probable sediment source, consistent with shoreline retreat of 7–10 m/yr along the northern coast and 3–8 m/yr along the western coast of the IGoT, primarily driven by subaerial and subaqueous delta subsidence as well as rapid sea-level rise (Figures 1b and 1c; Bidorn et al., 2021; Sok et al., 2022). In the Chao Phraya Delta, with a gentle slope (1 m/km) and 1.5–2.5 m tidal ranges (Bidorn et al., 2021), subaqueous erosion can extend 1.5–2.5 km offshore (Saito, 2000), similar to the abandoned Yellow River Delta, where subaqueous erosion redistributes 500 Mt/yr of sediment, particularly during storms (Zhu et al., 2024). In the IGoT, evidence from sediment cores, such as abnormally low excess ^{210}Pb layers interrupting successions of normally high excess ^{210}Pb , indicating rapid storm-driven deposition of older eroded material, supported by local accounts from coastal villages like the Ban Khun Samut Chin (Burnett et al., 2023). Moreover, the loss of mangroves—converted to aquaculture—has further weakened natural defenses (Figure 1d; Bidorn et al., 2021). The remaining mangroves cannot sustain accretion under persistent rapid sea-level rise (>0.6 cm/yr; Saintilan et al., 2020), exposing low-lying coasts to rapid erosion. While efforts like mangrove reforestation programs, engineered coastal protection structures, and regulation-driven reduction in groundwater pumping aim to counteract this, their impact has been limited, with only marginally mangrove recovery since 2000, indicating a slight deceleration of coastal erosion (Figure 1d; Bidorn et al., 2021; Chawalit et al., 2025). Additional erosion may stem from industrial development (e.g., in the eastern Chao Phraya Delta) and abandoned aquaculture areas. However, these sediment sources are less well constrained and may have a more localized impact.

Irrespective of the type of sediment, coastal erosion is the dominant contributor to terrigenous sediment accumulation in the IGoT, particularly after 1975. This is supported by an increase in the coastal-to-riverine sediment ratio from 2.1 to 4.4 and a 40% increase in terrestrial OC input since the 1980s in a nearby sediment core (Liu et al., 2025), despite a concurrent decline in riverine sediment flux.

4.2. Burial Efficiency of OC_{river} and $OC_{coastal}$ in the IGoT

Coastal erosion and riverine input likely deliver different forms of terrigenous OC to the marine environment, although their ultimate fates remain underexplored. In the IGoT, the five main rivers contributed an average OC_{river} flux of 186.9 ± 5.4 Gg/yr post-1975, yet only 62.7 ± 6.3 Gg/yr was deposited in the region (Table 1). The sediment budget suggests that most riverine sediments are ultimately buried locally with minimal potential contributions from distant rivers, yielding an OC_{river} burial efficiency of $33.5 \pm 2.8\%$. This is about double the 15% estimate for the GoT based on OC_{river} loading (Lin et al., 2023), which lacked a sediment budget accounting for spatial differences in MAR, potentially underestimating OC_{river} burial efficiencies in continental margins. It also highly surpasses the global average of $\sim 21\%$ estimated for continental margins (Burdige, 2005) and the 18.2% reported for the adjacent Sunda Shelf off the Malay Peninsula (Wei et al., 2024). This relatively higher OC_{river} burial efficiency likely reflects the generally weak hydrodynamic conditions in the IGoT, which facilitates rapid local OC_{river} deposition and reduces lateral OC_{river} transport and degradation in suspension-deposition loops.

Coastal erosion was calculated to contribute 452.9 ± 142.8 Gg/yr of $OC_{coastal}$ to the IGoT (Table 1), but only 76.3 ± 7.6 Gg/yr was deposited in the region, resulting in a burial efficiency of $16.8 \pm 5.5\%$, about half of that calculated for OC_{river} . This lower burial efficiency stems from several factors. OC_{river} burial efficiency is calculated relative to its content in suspended and bedload river sediments, which has already undergone degradation and selective preservation during soil erosion and riverine transport (Wei et al., 2020). In contrast, $OC_{coastal}$ burial efficiency compares its burial flux in marine sediments to its original stock in coastal ecosystems (mainly topsoil, leaf litter and reworked roots in wetland deposits), which is generally less processed and more susceptible to decomposition in oxic marine settings (Kida & Fujitake, 2020; Kristensen et al., 2008). In addition, vegetated coastal wetland ecosystems with their muddy substrates offer largely anaerobic, low-light conditions that promote OC preservation. Thus, when eroded $OC_{coastal}$ enters the well-oxygenated, highly translucent coastal waters, aerobic decomposition and photodegradation is facilitated (Dittmar et al., 2006). Thus, the low burial efficiency of $OC_{coastal}$ in the IGoT primarily results from its generally fresh and less-processed nature, greater exposure to oxygen and loss of stabilizing mechanisms after erosion.

4.3. Implications for Global Carbon Dynamics

Coastal erosion is increasingly recognized for its significant impact on global carbon dynamics, particularly in the Arctic where coastal permafrost erosion releases $\sim 22 \pm 8$ Tg C/yr of greenhouse gases (Vonk et al., 2012). Yet, its impact on sedimentary OC dynamics in tropical low-lying areas, particularly under a scenario of rapid sea-level rise and intensified human activities, remain largely unknown. While the immense OC storage capacity of above- and belowground mangrove system has been demonstrated, most work has focused on deforestation (Atwood et al., 2017; Donato et al., 2011), with coastal erosion only recently acknowledged as the second-largest threat to these carbon sinks (e.g., Adame et al., 2021). Nevertheless, the fate of this terrestrial OC in marine environments and the resulting greenhouse gas emissions (or other feedback mechanisms) are poorly constrained. This study highlights the dominance of regional coastal erosion over riverine sediment discharge into the IGoT, contributing 2.1 \times and 4.4 \times more sediments than rivers pre-1975 and post-1975, respectively. This implies that coastal erosion can in part offset sediment loss from upstream damming (Bidorn et al., 2023), but comes at a major carbon cost: $83.2 \pm 5.5\%$ loss of $OC_{coastal}$ that was originally stabilized within the eroded coastal wetlands. This underscores the vulnerability of $OC_{coastal}$ to rapid erosion, export and degradation, driven by climatic changes (e.g., global warming, rising sea level, increasing storm intensity, changing monsoon dynamics and circulation changes) as well as human land-use and river-management practices (e.g., water management, channel mining, groundwater extraction, and coastal ecosystem conversion).

Southeast Asia and tropical Oceania harbor the largest above- and belowground mangrove OC stocks globally ($\sim 68\%$; Thorhaug et al., 2020; Zhang et al., 2024) and are projected to experience the largest future OC loss, primarily driven by deforestation for agriculture and aquaculture purposes as well as coastal erosion (Adame et al., 2021; Atwood et al., 2017; Chatting et al., 2022). Thus, resolving $OC_{coastal}$ dynamics in this region is particularly important. To our knowledge, this study is the first to estimate the burial efficiency of $OC_{coastal}$ released by coastal erosion. As such, we cannot directly compare our estimate for the IGoT with other tropical systems. Coastal ocean sedimentation and erosion dynamics are complex and differ regionally in response to the multitude of intensifying environmental pressures (Syvitski et al., 2009). The IGoT is semi-enclosed and shallow,

resulting in limited wave energy, which affects sediment transport and deposition that ultimately influence OC_{coastal} burial efficiency. Three of the world's seven largest river-dominated deltas—Ganges-Brahmaputra-Meghna, Mekong, and Irrawaddy—are near the IGoT, each exhibits different coastal erosion and OC burial patterns. The Bengal Shelf, off the Ganges-Brahmaputra-Meghna, sees high sediment deposition (up to 8.6 cm/yr; Kuehl et al., 1989) and nearly 100% terrestrial OC burial efficiency (Galy et al., 2007), which has kept erosion low (highest rates 0.1–0.2 km²/yr; Haque et al., 2024). The Irrawaddy experiences coastal accretion (4.4 km²/yr; Chen et al., 2020), but terrestrial OC burial efficiency in the Andaman Sea is lower (~36%; Furuichi et al., 2009). In contrast, the Mekong Delta suffers severe coastal erosion (0.7–2.3 km²/yr; Anthony et al., 2015), with terrestrial OC burial in the South China Sea (~25%; Lin et al., 2023) lower than in these systems and the IGoT. Based on the combination of low coastal erosion rates and medium to high terrestrial OC burial efficiency on the Bengal Shelf and in the Andaman Sea, we expect relatively high OC_{coastal} burial efficiencies there. In contrast, OC_{coastal} burial efficiencies are likely low in the Mekong-South China Sea system, a shallow shelf similar to the IGoT. Beyond Southeast Asia, coastal erosion threatens mangrove systems along the North Brazilian Shelf and tropical NW Atlantic, which represent ~18% of global mangrove OC stocks (Rovai et al., 2022; Thorhaug et al., 2019). The Amazon-Guianas coast experiences intense wave-driven erosion, moving ~250 Mt/yr of sediment from mangrove fringes to the subaqueous mudbelt (Allison & Lee, 2004), where terrestrial OC burial efficiency (~30%–35%; Aller et al., 1996) is similar to the IGoT, thus we expect comparable OC_{coastal} burial efficiency as well.

Global marine mangroves store $3,025 \pm 345$ Tg of soil OC (Zhang et al., 2024) but are declining at ~1.9% (0.7%–3%) annually (Pendleton et al., 2012), due to conversion for agri/aquaculture, clearing, extreme climatic events and human settlements (Adame et al., 2021). Using the loss proportion of eroded OC_{coastal} ($83.2 \pm 5.5\%$; primarily mangrove OC) from this study, we estimate CO₂ emissions from global marine mangrove loss at 175.3 ± 60.8 Tg/yr, slightly lower than Pendleton et al.'s (2012) estimate of 240 Tg/yr CO₂ (90–450 Tg/yr). This comparison suggests our IGoT-based burial efficiency offers a conservative estimate, although more regional data are needed to better understand the role of mangrove OC loss response to direct land use change/forest destruction versus driven by coastal erosion. Among blue carbon ecosystems, mangroves exhibit the highest near-surface carbon loss flux (240 Tg/yr) compared to tidal marshes (60 Tg/yr) and seagrasses (150 Tg/yr), totaling ~450 Tg/yr of CO₂ emission globally (Pendleton et al., 2012). These findings, combined with this study, underscore the urgent need for coastal management strategies to protect these critical “blue carbon” sinks and decisively mitigate the impacts of global warming. As coastal erosion accelerates, preserving coastal ecosystems is essential for maintaining regional carbon balance and safeguarding against broader, often irreversible, environmental and social consequences.

Data Availability Statement

Data reported in this study is being archived in the PANGAEA (Wei, 2025a, 2025b, 2025c).

Acknowledgments

The research was funded by the DFG Cluster of Excellence (EXC-2077-390741603, “The Ocean Floor—Earth's Uncharted Interface”), the Helmholtz Association (Alfred Wegener Institute Helmholtz Centre for Polar and Marine Research, Helmholtz Research Program “Changing Earth—Sustaining our Future” in PoF IV), and the China Post-doctoral Science Foundation (2021M692410). We thank Prof. William Burnett and two anonymous reviewers for their constructive comments that helped improve the manuscript. Open Access funding enabled and organized by Projekt DEAL.

References

- Adame, M. F., Connolly, R. M., Turschwell, M. P., Lovelock, C. E., Fatoyinbo, T., Lagomasino, D., et al. (2021). Future carbon emissions from global mangrove forest loss. *Global Change Biology*, 27(12), 2856–2866. <https://doi.org/10.1111/gcb.15571>
- Aller, R. C., Blair, N. E., Xia, Q., & Rude, P. D. (1996). Remineralization rates, recycling, and storage of carbon in Amazon shelf sediments. *Continental Shelf Research*, 16(5–6), 753–786. [https://doi.org/10.1016/0278-4343\(95\)00046-1](https://doi.org/10.1016/0278-4343(95)00046-1)
- Allison, M. A., & Lee, M. T. (2004). Sediment exchange between Amazon mudbanks and shore-fringing mangroves in French Guiana. *Marine Geology*, 208(2–4), 169–190. <https://doi.org/10.1016/j.margeo.2004.04.026>
- Anthony, E. J., Brunier, G., Besset, M., Goichot, M., Dussouillez, P., & Nguyen, V. L. (2015). Linking rapid erosion of the Mekong River delta to human activities. *Scientific Reports*, 5, 1–12. <https://doi.org/10.1038/srep14745>
- Anutaliya, A. (2023). Surface circulation in the Gulf of Thailand from remotely sensed observations: Seasonal and interannual timescales. *Ocean Science*, 19(2), 335–350. <https://doi.org/10.5194/os-19-335-2023>
- Atwood, T. B., Connolly, R. M., Almahasheer, H., Carnell, P. E., Duarte, C. M., Lewis, C. J. E., et al. (2017). Global patterns in mangrove soil carbon stocks and losses. *Nature Climate Change*, 7(7), 523–528. <https://doi.org/10.1038/nclimate3326>
- Bai, Y., Hu, L., Wu, B., Qiao, S., Fan, D., Liu, S., et al. (2021). Impact of source variability and hydrodynamic forces on the distribution, transport, and burial of sedimentary organic matter in a tropical coastal margin: The Gulf of Thailand. *Journal of Geophysical Research: Biogeosciences*, 126(9), e2021JG006434. <https://doi.org/10.1029/2021JG006434>
- Barnard, P. L., Short, A. D., Harley, M. D., Splinter, K. D., Vitousek, S., Turner, I. L., et al. (2015). Coastal vulnerability across the Pacific dominated by El Niño/Southern Oscillation. *Nature Geoscience*, 8(10), 801–807. <https://doi.org/10.1038/ngeo2539>
- Bidorn, B., Namsai, M., Charoenlerkthawin, W., & Bidorn, K. (2023). Recent changes in sediment supply to the Chao Phraya delta. In *Proceedings of the IAHR World Congress, (August 2013)* (pp. 11–25). https://doi.org/10.3850/978-90-833476-1-5_iahr40wc-p0943-cd

- Bidorn, B., Sok, K., Bidorn, K., & Burnett, W. C. (2021). An analysis of the factors responsible for the shoreline retreat of the Chao Phraya Delta (Thailand). *Science of the Total Environment*, 769, 145253. <https://doi.org/10.1016/j.scitotenv.2021.145253>
- Boonphakdee, T., Kasai, A., Fujiwara, T., Sawangwong, P., & Cheevaporn, V. (2008). Combined stable carbon isotope and C/N ratios as indicators of source and fate of organic matter in the Bangpakong River Estuary, Thailand. *Environment*.
- Boonyatumanond, R., Wattayakorn, G., Amano, A., Inouchi, Y., & Takada, H. (2007). Reconstruction of pollution history of organic contaminants in the upper Gulf of Thailand by using sediment cores: First report from Tropical Asia Core (TACO) project. *Marine Pollution Bulletin*, 54(5), 554–565. <https://doi.org/10.1016/j.marpolbul.2006.12.007>
- Bosch, C., Andersson, A., Krusá, M., Bandh, C., Hovorková, I., Klánová, J., et al. (2015). Source apportionment of polycyclic aromatic hydrocarbons in central European soils with compound-specific triple isotopes ($\delta^{13}\text{C}$, $\Delta^{14}\text{C}$, and $\delta^2\text{H}$). *Environmental Science & Technology*, 49(13), 7657–7665. <https://doi.org/10.1021/acs.est.5b01190>
- Burdige, D. J. (2005). Burial of terrestrial organic matter in marine sediments: A re-assessment. *Global Biogeochemical Cycles*, 19(4), 1–7. <https://doi.org/10.1029/2004GB002368>
- Burnett, W. C., Bidorn, B., & Wang, Y. (2023). Can ^{210}Pb be used as a paleo-storm proxy? *Quaternary Science Reviews*, 315, 108242. <https://doi.org/10.1016/j.quascirev.2023.108242>
- Chaisanguansuk, P., Phantuwoongraj, S., Jirapinyakul, A., & Assawincharnokij, T. (2023). Preliminary study on microplastic abundance in mangrove sediment cores at Mae Klong River, upper Gulf of Thailand. *Frontiers in Environmental Science*, 11, 1–12. <https://doi.org/10.3389/fenvs.2023.1134988>
- Chatting, M., Al-Maslami, I., Walton, M., Skov, M. W., Kennedy, H., Husrevoglu, Y. S., & Le Vay, L. (2022). Future mangrove carbon storage under climate change and deforestation. *Frontiers in Marine Science*, 9, 1–14. <https://doi.org/10.3389/fmars.2022.781876>
- Chawalit, C., Boonpook, W., Sithi, A., Torsri, K., Kamthongkiat, D., Tan, Y., et al. (2025). Geoinformatics and machine learning for shoreline change monitoring: A 35-year analysis of coastal erosion in the Upper Gulf of Thailand. *ISPRS International Journal of Geo-Information*, 14(2), 94. <https://doi.org/10.3390/ijgi14020094>
- Cheevaporn, V., Jacinto, G. S., & San Diego-McGlone, M. L. (1994). History of heavy metal contamination in Bang Pakong Estuary, Thailand. *Journal of the Science Society of Thailand*, 20, 9–22.
- Chen, D., Li, X., Saito, Y., Liu, J. P., Duan, Y., Liu, S., & Zhang, L. (2020). Recent evolution of the Irrawaddy (Ayeyarwady) delta and the impacts of anthropogenic activities: A review and remote sensing survey. *Geomorphology*, 365, 107231. <https://doi.org/10.1016/j.geomorph.2020.107231>
- Darby, S. E., Hackney, C. R., Leyland, J., Kumm, M., Lauri, H., Parsons, D. R., et al. (2016). Fluvial sediment supply to a mega-delta reduced by shifting tropical-cyclone activity. *Nature*, 539(7628), 276–279. <https://doi.org/10.1038/nature19809>
- Dittmar, T., Hertkorn, N., Kattner, G., & Lara, R. J. (2006). Mangroves, a major source of dissolved organic carbon to the oceans. *Global Biogeochemical Cycles*, 20(1), 1–7. <https://doi.org/10.1029/2005GB002570>
- Donato, D. C., Kauffman, J. B., Murdiyarso, D., Kurnianto, S., Stidham, M., & Kanninen, M. (2011). Mangroves among the most carbon-rich forests in the tropics. *Nature Geoscience*, 4(5), 293–297. <https://doi.org/10.1038/ngeo1123>
- Duarte, C. M., Losada, I. J., Hendriks, I. E., Mazarrasa, I., & Marbà, N. (2013). The role of coastal plant communities for climate change mitigation and adaptation. *Nature Climate Change*, 3(11), 961–968. <https://doi.org/10.1038/nclimate1970>
- Furuichi, T., Win, Z., & Wasson, R. J. (2009). Discharge and suspended sediment transport in the Ayeyarwady River, Myanmar: Centennial and decadal changes. *Hydrological Processes*, 23(11), 1631–1641. <https://doi.org/10.1002/hyp.7295>
- Galy, V., France-Lanord, C., Beyssac, O., Faure, P., Kudrass, H., & Palhol, F. (2007). Efficient organic carbon burial in the Bengal fan sustained by the Himalayan erosional system. *Nature*, 450(7168), 407–410. <https://doi.org/10.1038/nature06273>
- Giri, C., Ochieng, E., Tieszen, L. L., Zhu, Z., Singh, A., Loveland, T., et al. (2011). Status and distribution of mangrove forests of the world using Earth observation satellite data (version 1.3, updated by UNEP-WCMC). *Global Ecology and Biogeography*, 20(1), 154–159. <https://doi.org/10.1111/j.1466-8238.2010.00584.x>
- Guo, Y., Qiao, S., Shi, X., Wu, B., Yuan, L., Ren, Y., et al. (2018). Variation trend and contamination source of heavy metals in sediments from estuary area of Bangkok Bay in the past century. *Marine Geology & Quaternary Geology*, 39(2).
- Haque, M. M., Haque, M., & Ghosh, M. K. (2024). The coastal dynamics of the central Ganges–Brahmaputra–Meghna delta coast, Bangladesh: Implications for coastal development and sustainability. *Journal of Coastal Conservation*, 28(1), 29. <https://doi.org/10.1007/s11852-024-01032-7>
- Hungspreugs, M., Utoomprukporn, W., Sompongchaiyakul, P., & Heungkraksa, W. (2002). Possible impact of dam reservoirs and river diversions on material fluxes to the Gulf of Thailand. *Marine Chemistry*, 79(3–4), 185–191. [https://doi.org/10.1016/S0304-4203\(02\)00063-4](https://doi.org/10.1016/S0304-4203(02)00063-4)
- Imlamai, P., Worachananant, S., & Phaksopa, J. (2023). Monitoring study of coastal morphological change from coastal engineering structures at Mrigadayavan Palace, Phetchaburi province using geo-informatics. *Burapha Science Journal*.
- JICA. (2000). *The feasibility study on mangrove revival and extension project in the kingdom of Thailand. Draft final report*. Ministry of Agriculture.
- Kessarkar, P. M., Rao, V. P., Shynu, R., Mehra, P., & Viegas, B. E. (2010). The nature and distribution of particulate matter in the Mandovi estuary, central west coast of India. *Estuaries and Coasts*, 33(1), 30–44. <https://doi.org/10.1007/s12237-009-9226-0>
- Kida, M., & Fujitake, N. (2020). Organic carbon stabilization mechanisms in mangrove soils: A review. *Forests*, 11(9), 1–15. <https://doi.org/10.3390/f11090981>
- Kristensen, E., Bouillon, S., Dittmar, T., & Marchand, C. (2008). Organic carbon dynamics in mangrove ecosystems: A review. *Aquatic Botany*, 89(2), 201–219. <https://doi.org/10.1016/j.aquabot.2007.12.005>
- Kuehl, S. A., Hariu, T. M., & Moore, W. S. (1989). Shelf sedimentation off the Ganges-Brahmaputra river system: Evidence for sediment bypassing to the Bengal fan. *Geology*, 17(12), 1132–1135. [https://doi.org/10.1130/0091-7613\(1989\)017<1132:SSOTGB>2.3.CO;2](https://doi.org/10.1130/0091-7613(1989)017<1132:SSOTGB>2.3.CO;2)
- Lin, B., Liu, Z., Zhao, M., Sompongchaiyakul, P., Zhang, H., Blattmann, T. M., et al. (2023). Compositions and sources of sedimentary organic carbon on the tropical epicontinental sea. *Geochimica et Cosmochimica Acta*, 351, 32–44. <https://doi.org/10.1016/j.gca.2023.04.030>
- Liu, M., Bai, Y., Jiang, L., Hu, L., Wu, B., Qiao, S., et al. (2025). Changes in accumulation of land-based organic matter under recent climate change and anthropogenic impact: A tropical coastal perspective. *Catena*, 248, 108611. <https://doi.org/10.1016/j.catena.2024.108611>
- Liu, M., Raymond, P. A., Lauerwald, R., Zhang, Q., Trapp-Müller, G., Davis, K. L., et al. (2024). Global riverine land-to-ocean carbon export constrained by observations and multi-model assessment. *Nature Geoscience*, 17(9), 896–904. <https://doi.org/10.1038/s41561-024-01524-z>
- Liu, Z., Liu, X., & Li, X. (2011). Discussion on smectite formation in South China Sea sediments. *Quaternary Sciences*, 31(2). <https://doi.org/10.3969/j.issn.1001-7410.2011.02.01>
- Liu, Z., Zhao, Y., Colin, C., Stattegger, K., Wiesner, M. G., Huh, C. A., et al. (2016). Source-to-sink transport processes of fluvial sediments in the South China Sea. *Earth-Science Reviews*, 153, 238–273. <https://doi.org/10.1016/j.earscirev.2015.08.005>

- Lorphensri, O., Ladawadee, A., & Dhammasarn, S. (2011). Review of groundwater management and land subsidence in Bangkok, Thailand. In *Groundwater and subsurface environments: Human impacts in Asian coastal cities* (pp. 127–142).
- Martínez, M. L., Intralawan, A., Vázquez, G., Pérez-Maqueo, O., Sutton, P., & Landgrave, R. (2007). The coasts of our world: Ecological, economic and social importance. *Ecological Economics*, 63(2–3), 254–272. <https://doi.org/10.1016/j.ecolecon.2006.10.022>
- Mentaschi, L., Voudoukas, M. I., Pekel, J. F., Voukouvalas, E., & Feyen, L. (2018). Global long-term observations of coastal erosion and accretion. *Scientific Reports*, 8(1), 1–11. <https://doi.org/10.1038/s41598-018-30904-w>
- Narman, L. S. (2020). *Carbon transfer in the western South China Sea - biogeochemical perspectives on organic carbon pools in surface sediments, from surface to burial*. PhD. Thesis. Heriot Watt University.
- Nutalaya, P. (1996). Coastal erosion in the Gulf of Thailand. *Geojournal*, 38(3), 283–300. <https://doi.org/10.1007/BF00204721>
- Pa'suya, M. F., Peter, B. N., Md Din, A. H., & Mohd Omar, K. (2015). Sea surface current in the gulf of Thailand based on Nineteen years altimetric data and GPS tracked drifting buoy. In *ACRS 2015—36th Asian Conference on Remote Sensing: Fostering Resilient Growth in Asia, Proceedings*.
- Pendleton, L., Donato, D. C., Murray, B. C., Crooks, S., Jenkins, W. A., Sifleet, S., et al. (2012). Estimating global “blue carbon” emissions from conversion and degradation of vegetated coastal ecosystems. *PLoS One*, 7(9), e43542. <https://doi.org/10.1371/journal.pone.0043542>
- Phien-wej, N., Giao, P. H., & Nutalaya, P. (2006). Land subsidence in Bangkok, Thailand. *Engineering Geology*, 82(4), 187–201. <https://doi.org/10.1016/j.enggeo.2005.10.004>
- Qiao, S., Shi, X., Fang, X., Liu, S., Kornkanitnan, N., Gao, J., et al. (2015). Heavy metal and clay mineral analyses in the sediments of Upper Gulf of Thailand and their implications on sedimentary provenance and dispersion pattern. *Journal of Asian Earth Sciences*, 114, 488–496. <https://doi.org/10.1016/j.jseaes.2015.04.043>
- Rovai, A. S., Twilley, R. R., Worthington, T. A., & Riul, P. (2022). Brazilian Mangroves: Blue carbon hotspots of national and global relevance to natural climate solutions. *Frontiers in Forests and Global Change*, 4. <https://doi.org/10.3389/ffgc.2021.787533>
- Saintilan, N., Khan, N. S., Ashe, E., Kelleway, J. J., Rogers, K., Woodroffe, C. D., & Horton, B. P. (2020). Thresholds of mangrove survival under rapid sea level rise. *Science*, 368(6495), 1118–1121. <https://doi.org/10.1126/science.aba2656>
- Saito, Y. (2000). Deltas in Southeast and East Asia: Their evolution and current problems. In N. Mimura & H. Yokoki (Eds.), *Global Change and Asia Pacific Coasts. Kobe, Japan: APN/SURVAS/LOICZ Joint Conference on Coastal Impacts of Climate Change and Adaptation in the Asia-Pacific Region*.
- Schlitzer, R. (2018). Ocean data view.
- Shi, X., Liu, S., Fang, X., Qiao, S., Khokiatwong, S., & Kornkanitnan, N. (2015). Distribution of clay minerals in surface sediments of the Western Gulf of Thailand: Sources and transport patterns. *Journal of Asian Earth Sciences*, 105, 390–398. <https://doi.org/10.1016/j.jseaes.2015.02.005>
- Sok, K., Bidorn, B., Burnett, W. C., Sasaki, J., & Sola, P. (2022). Seven decades of shoreline changes along a muddy mangrove coastline of the Upper Gulf of Thailand. *Earth Surface Processes and Landforms*, 47(6), 1425–1438. <https://doi.org/10.1002/esp.5324>
- Sompongchaiyakul, P., Bureekul, S., & Sombatjinda, S. (2019). Impact of natural gas exploration and production on mercury concentrations in surface sediment of the Gulf of Thailand. In *Society of Petroleum Engineers—Abu Dhabi International Petroleum Exhibition and Conference 2018, ADIPEC 2018*. <https://doi.org/10.2118/192739-ms>
- Srisuksawad, K., Porntepkasemsan, B., Nouchpramool, S., Yamkate, P., Carpenter, R., Peterson, M. L., & Hamilton, T. (1997). Radionuclide activities, geochemistry, and accumulation rates of sediments in the Gulf of Thailand. *Continental Shelf Research*, 17(8), 925–965. [https://doi.org/10.1016/s0278-4343\(96\)00065-9](https://doi.org/10.1016/s0278-4343(96)00065-9)
- Syvitski, J., Ángel, J. R., Saito, Y., Overeem, I., Vörösmarty, C. J., Wang, H., & Olago, D. (2022). Earth's sediment cycle during the Anthropocene. *Nature Reviews Earth & Environment*, 3(3), 179–196. <https://doi.org/10.1038/s43017-021-00253-w>
- Syvitski, J. P. M., Kettner, A. J., Overeem, I., Hutton, E. W. H., Hannon, M. T., Brakenridge, G. R., et al. (2009). Sinking deltas due to human activities. *Nature Geoscience*, 2(10), 681–686. <https://doi.org/10.1038/ngeo629>
- Tegler, L. A., Horner, T. J., Galy, V., Bent, S. M., Wang, Y., Kim, H. H., et al. (2024). Distribution and drivers of organic carbon sedimentation along the continental margins. *AGU Advances*, 5(4), 1–22. <https://doi.org/10.1029/2023AV001000>
- Thimdee, W., Deen, G., Sangrungruang, C., Nishioka, J., & Matsunaga, K. (2003). Sources and fate of organic matter in Khung Krabaen Bay (Thailand) as traced by $\delta^{13}\text{C}$ and C/N atomic ratios. *Wetlands*, 23(4), 729–738. [https://doi.org/10.1672/0277-5212\(2003\)023\[0729:safoom\]2.0.co;2](https://doi.org/10.1672/0277-5212(2003)023[0729:safoom]2.0.co;2)
- Thorhaug, A., Gallagher, J. B., Kiswara, W., Prathep, A., Huang, X., Yap, T. K., et al. (2020). Coastal and estuarine blue carbon stocks in the greater Southeast Asia region: Seagrasses and mangroves per nation and sum of total. *Marine Pollution Bulletin*, 160, 111168. <https://doi.org/10.1016/j.marpolbul.2020.111168>
- Thorhaug, A. L., Poulos, H. M., López-Portillo, J., Barr, J., Lara-Domínguez, A. L., Ku, T. C., & Berlyn, G. P. (2019). Gulf of Mexico estuarine blue carbon stock, extent and flux: Mangroves, marshes, and seagrasses: A North American hotspot. *Science of the Total Environment*, 653, 1253–1261. <https://doi.org/10.1016/j.scitotenv.2018.10.011>
- Ubonyaem, T., Bureekul, S., Charoenpong, C., & Sompongchaiyakul, P. (2023). Variation of mercury in 4 major estuaries in the Gulf of Thailand during wet season. *Continental Shelf Research*, 267(August), 105105. <https://doi.org/10.1016/j.csr.2023.105105>
- Vongvisessomjai, S., Polsi, R., Manotham, C., Srisaengthong, D., & Charulukkana, S. (1996). Coastal erosion in the Gulf of Thailand. In J. D. Milliman & B. U. Haq (Eds.), *Sea-level rise and coastal subsidence* (Vol. 2, pp. 226–230). Springer Science+Business Media Dordrecht.
- Vonk, J. E., Sanchez-Garcia, L., Van Dongen, B. E., Alling, V., Kosmach, D., Charkin, A., et al. (2012). Activation of old carbon by erosion of coastal and subsea permafrost in Arctic Siberia. *Nature*, 489(7414), 137–140. <https://doi.org/10.1038/nature11392>
- Wagner, T., Clift, P., Dommain, R., Hanebuth, T., Novico, F., Shaw, T., et al. (2024). The Sunda region in maritime Southeast Asia—A tropical window into global carbon-climate relationships, hominin evolution, and ecosystem feedback since the Plio-Pleistocene. *PAGES Magazine*, 32, 68–69. <https://doi.org/10.22498/pages.32.2.68>
- Wei, B. (2025a). Measured and estimated discharge and suspended sediment flux of the Chao Phraya River, along with the Phetchaburi, Mae Klong, Tha Chin, and Bang Pakong rivers during 1912–2020 [Dataset]. *PANGAEA*. <https://doi.org/10.1594/PANGAEA.981111>
- Wei, B. (2025b). Geochemical properties of surface sediments in the inner Gulf of Thailand [Dataset]. *PANGAEA*. <https://doi.org/10.1594/PANGAEA.981135>
- Wei, B. (2025c). Reported linear sedimentation (LSR) and mass accumulation rate (MAR), as well as corrected mean MAR pre-1975 and post-1975 in the inner Gulf of Thailand [Dataset]. *PANGAEA*. <https://doi.org/10.1594/PANGAEA.981145>
- Wei, B., Kusch, S., Wu, J., Shaari, H., Mollenhauer, G., & Jia, G. (2024). River mouths are hotspots for terrestrial organic carbon burial on the Sunda Shelf: Implications for tropical coastal carbon sequestration. *Geochimica et Cosmochimica Acta*, 387(November), 1–11. <https://doi.org/10.1016/j.gca.2024.10.037>

- Wei, B., Mollenhauer, G., Hefter, J., Grotheer, H., & Jia, G. (2020). Dispersal and aging of terrigenous organic matter in the Pearl river estuary and the northern South China Sea Shelf. *Geochimica et Cosmochimica Acta*, 282, 324–339. <https://doi.org/10.1016/j.gca.2020.04.032>
- Windom, H. L., Silpipat, S., Chanpongsang, A., Smith, R. G., & Hungspreugs, M. (1984). Trace metal composition of and accumulation rates of sediments in the Upper Gulf of Thailand. *Estuarine, Coastal and Shelf Science*, 19(2), 133–142. [https://doi.org/10.1016/0272-7714\(84\)90060-X](https://doi.org/10.1016/0272-7714(84)90060-X)
- Wu, B., Wu, X., Shi, X., Qiao, S., Liu, S., Hu, L., et al. (2020). Influences of tropical monsoon climatology on the delivery and dispersal of organic carbon over the Upper Gulf of Thailand. *Marine Geology*, 426(March), 106209. <https://doi.org/10.1016/j.margeo.2020.106209>
- Zhang, J., Gan, S., Yang, P., Zhou, J., Huang, X., Chen, H., et al. (2024). A global assessment of mangrove soil organic carbon sources and implications for blue carbon credit. *Nature Communications*, 15(1), 8994. <https://doi.org/10.1038/s41467-024-53413-z>
- Zhu, Q., Xing, F., Wang, Y. P., Syvitski, J., Overeem, I., Guo, J., et al. (2024). Hidden delta degradation due to fluvial sediment decline and intensified marine storms. *Science Advances*, 10(18). <https://doi.org/10.1126/sciadv.adk1698>

References From the Supporting Information

- Chaikaew, P., & Chavanich, S. (2017). Spatial variability and relationship of mangrove soil organic matter to organic carbon. *Applied and Environmental Soil Science*, 2017, 1–9. <https://doi.org/10.1155/2017/4010381>
- Chinfak, N., Charoenpong, C., Wu, Y., Zhang, G., Somphongchaiyakul, P., & Zhang, J. (2023). Dominance of land-derived organic matter in highly productive Bandon Bay, Thailand. *Continental Shelf Research*, 257, 104963. <https://doi.org/10.1016/j.csr.2023.104963>
- Hu, J., Pradit, S., Loh, P. S., Chen, Z., Guo, C., Le, T. P. Q., et al. (2024). Storage and dynamics of soil organic carbon in allochthonous-dominated and nitrogen-limited natural and planted mangrove forests in southern Thailand. *Marine Pollution Bulletin*, 200, 116064. <https://doi.org/10.1016/j.marpolbul.2024.116064>
- Matsui, N., Meepol, W., & Chukwamdee, J. (2015). Soil organic carbon in mangrove ecosystems with different vegetation and sedimentological conditions. *Journal of Marine Science and Engineering*, 3(4), 1404–1424. <https://doi.org/10.3390/jmse3041404>
- Srisunont, C., Jaiyen, T., Tenrungs, M., Likitchaikul, M., & Srisunont, T. (2017). Nutrient accumulation by Litterfall in mangrove forest at Klong Khone, Thailand. *Thammasat International Journal of Science and Technology*, 22(1).